Supporting Information for

Synthesis, characterization, and cytotoxic properties of mono- and di-nuclear cobalt(II)-polypridyl complexes

Arvin Eskandari,[a] Arunangshu Kundu,[b] Chunxin Lu,[c] Sushobhan Ghosh,[b]* and Kogularamanan Suntharalingam[a]*

[a] Department of Chemistry, King's College London, London, UK
[b] Department of Chemistry, Gauhati University, Guwahati, India
[c] Guangxi Colleges and Universities Key Laboratory of Beibu Gulf Oil and Natural Gas Resource Effective Utilization, Qinzhou University, Qinzhou 535011, China

* To whom correspondence should be addressed:
Email: kogularamanan.suntharalingam@kcl.ac.uk and sushobhan.iisc@gmail.com

Table of Content

Fig. S10 Inhibition of **1-** and **3-**mediated DNA cleavage by DNA minor and major groove binders and intercalators after 16 h incubation. (A) Lane 1: DNA only, Lane 2: DNA + **1** (10 μM) with 10 equivalents of ascorbic acid, Lane 3: DNA + **1** (10 μM) with 10 equivalents of ascorbic acid + methyl green (50 μM), Lane 4: DNA + **1** (10 μM) with 10 equivalents of ascorbic acid + DAPI (50 μM), Lane 5: DNA + **1** (10 μM) with 10 equivalents of ascorbic acid + TO (10 μM). (B) Lane 1: DNA only, Lane 2: DNA + **3** (10 μM) with 10 equivalents of ascorbic acid, Lane 3: DNA + **3** (10 μM) with 10 equivalents of ascorbic acid + methyl green (50 μM), Lane 4: DNA + **3** (10 μM) with 10 equivalents of ascorbic acid + DAPI (50 μM), Lane 5: DNA + **3** (10 μM) with 10 equivalents of ascorbic acid + TO (10 μM).

Fig. S11 Representative UV-Vis trace of **1** (50 μM) upon addition of ct-DNA (0 – 0.11 equivalence).

Fig. S12 Representative reciprocal plot of $D/\Delta\varepsilon_{ap}$ versus D of **1** (50 μM) upon addition of ct-DNA (0 – 0.11 eq.).

Fig. S13 Representative UV-Vis trace of **3** (50 μM) upon addition of ct-DNA (0 – 0.11 equivalence).

Fig. S14 Representative reciprocal plot of $D/\Delta\varepsilon_{ap}$ versus D of **3** (50 μM) upon addition of ct-DNA (0 – 0.11 eq.).

Table S5. Apparent binding constant (K_{bin}) and quenching constant (K_q) for the interaction of **1-3** with ct-DNA.

Fig. S15 Emission spectra for ethidium bromide (1 μM) bound to ct-DNA (20 μM) upon addition of aliquots of **1** (0-50 μM) and the corresponding F^o/F versus [Q] plot.

Fig. S16 Emission spectra for ethidium bromide (1 μM) bound to ct-DNA (20 μM) upon addition of aliquots of **2** (0-50 μM) and the corresponding F^o/F versus [Q] plot.

Fig. S17 Emission spectra for ethidium bromide (1 μM) bound to ct-DNA (20 μM) upon addition of aliquots of **3** (0-50 μM) and the corresponding F^o/F versus [Q] plot.

Fig. S18 Representative dose-response curves for the treatment of U2OS cells with **1-3** after 72 h incubation.

Fig. S19 Representative dose-response curves for the treatment of HepG2 cells with **1-3** after 72 h incubation.

Fig. S20 Representative dose-response curves for the treatment of GM07575 cells with **1-3** after 72 h incubation.

Fig. S21 Representative dose-response curves for the treatment of (A) U2OS or (B) HepG2 cells with cisplatin after 72 h incubation.

Fig. S22 Representative dose-response curves for the treatment of (A) U2OS or (B) HepG2 cells with carboplatin after 72 h incubation.

Fig. S23 Representative dose-response curves for the treatment of U2OS cells with $\mathbf{L^1}$, 4,4′-azopyridine, 4,4'-bipyridine, and $Co(NO_3)_2 \cdot 6H_2O$ after 72 h incubation.

Fig. S24 Representative dose-response curves for the treatment of HepG2 cells with $\mathbf{L^1}$, 4,4′-azopyridine, 4,4'-bipyridine, and $Co(NO_3)_2 \cdot 6H_2O$ after 72 h incubation.

Fig. S25 Cobalt content in U2OS cells treated with **1-3** (10 μM for 24 h).

Fig. S26 Representative dose-response curves for the treatment of U2OS cells with **4** in the presence of the p53 inhibitor, pifithrin-μ (10 μM) after 72 h incubation.

Fig. S27 Representative dose-response curves for the treatment of HepG2 cells with **4** in the presence of the p53 inhibitor, pifithrin-μ (10 μM) after 72 h incubation.

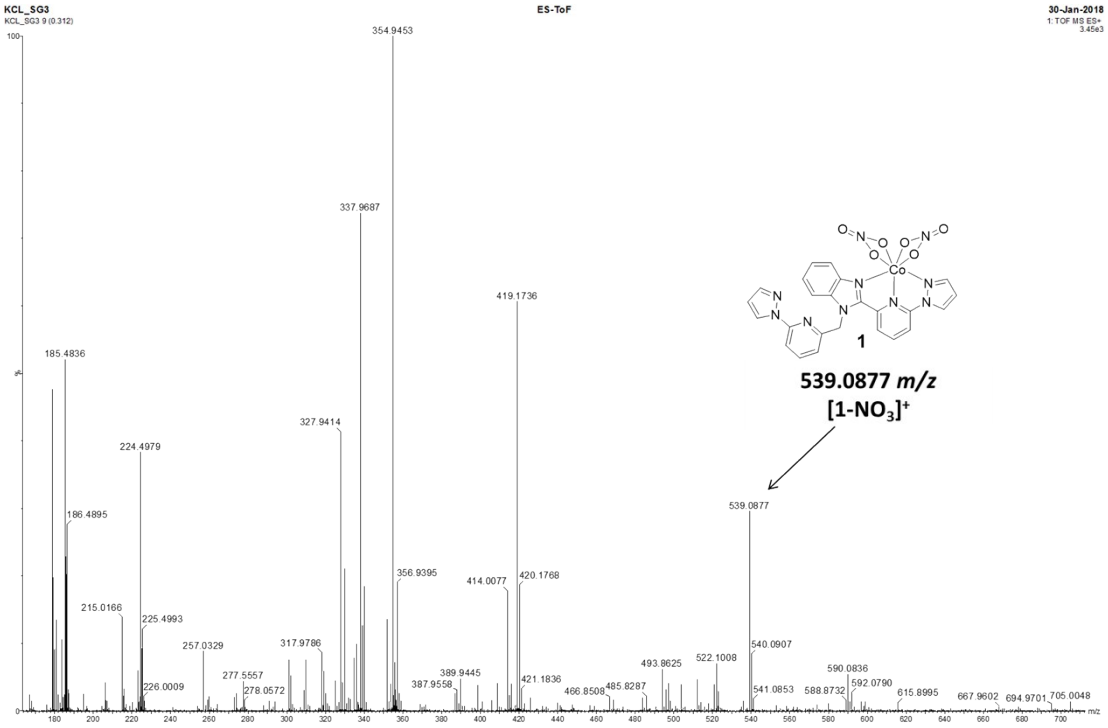

Fig. S1 High resolution ESI mass spectrum (positive mode) of **1**.

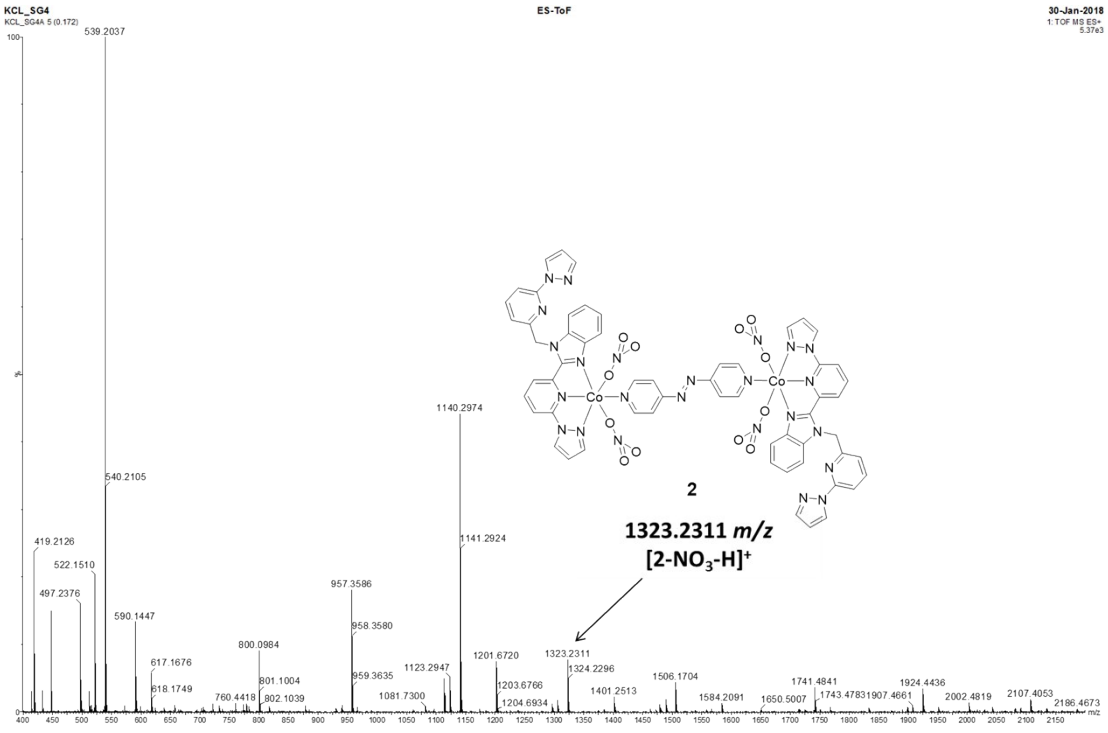

Fig. S2 High resolution ESI mass spectrum (positive mode) of **2**.

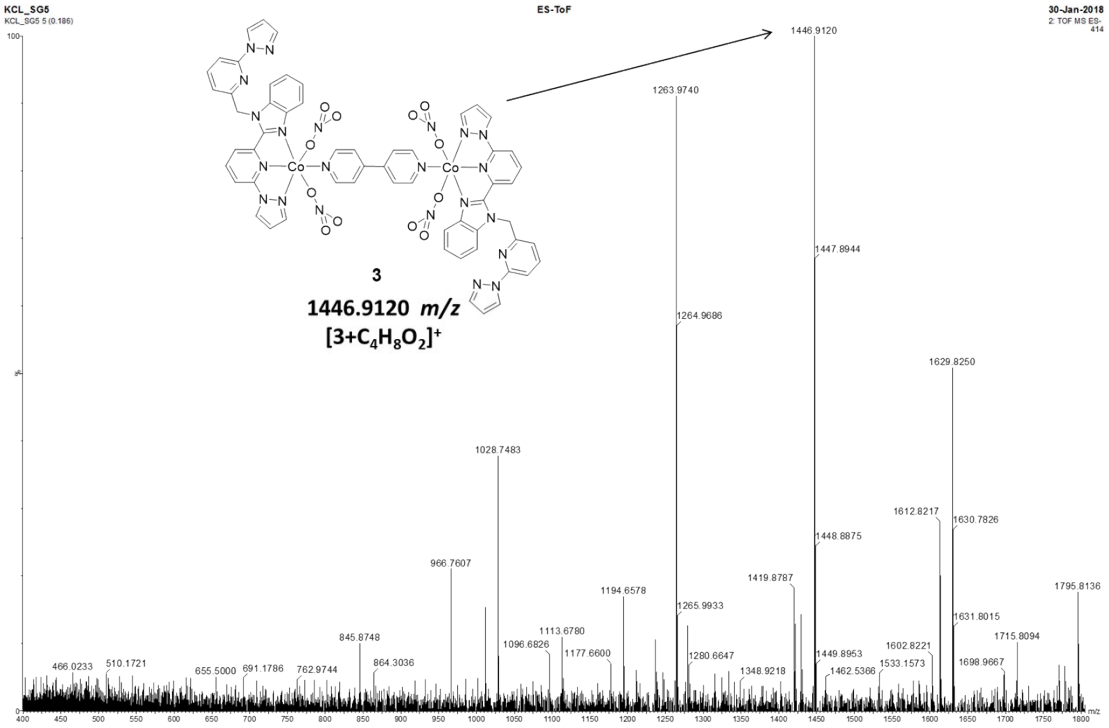

Fig. S3 High resolution ESI mass spectrum (negative mode) of **3**.

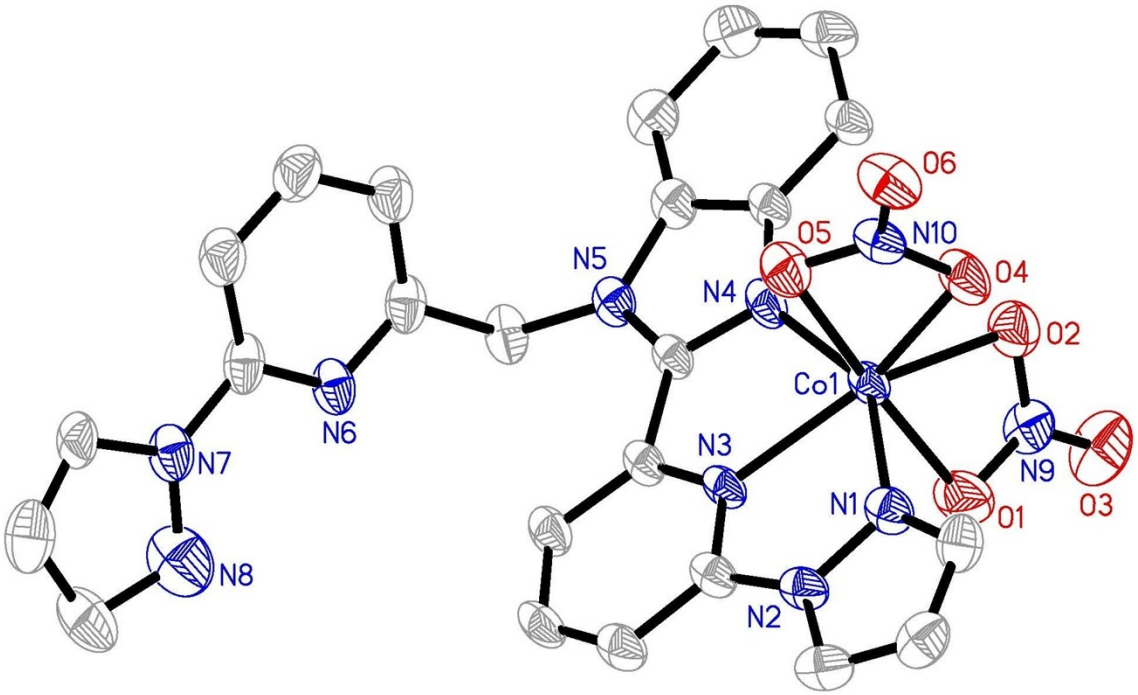

Fig. S4 X-ray structure of the mono-nuclear cobalt(II) complex, **1**. Ellipsoids are shown at 30% probability, O atoms are shown in red, C in grey, N in dark blue, and Co in light blue. H atoms have been omitted for clarity.

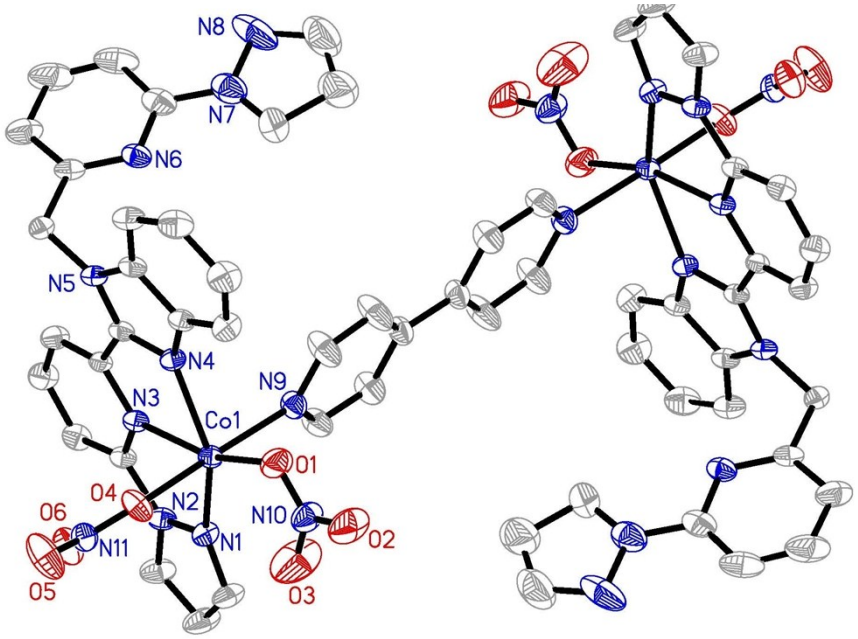

Fig. S5 X-ray structure of the di-nuclear cobalt(II) complex, **3**. Ellipsoids are shown at 30% probability, O atoms are shown in red, C in grey, N in dark blue, and Co in light blue. H atoms have been omitted for clarity.

Table S1. Crystallographic data of **1** and **3**.

	1	**3**
Formula	$C_{24}H_{18}CoN_{10}O_6$	$C_{58}H_{44}Co_2N_{22}O_{12}$
W	601.41	1359.01
Crystal system	triclinic	triclinic
Space group	*P*-1	*P-1*
a, Å	9.2563(5)	7.7180(12)
b, Å	9.5206(5)	14.973(2)
c, Å	15.9254(11)	15.659(2)
α, deg.	100.846(3)	106.656(8)
β, deg.	99.597(3)	99.420(8)
γ, deg.	108.983(2)	101.815(8)
V, Å^3	1263.54(13)	1648.5(4)
Z	2	1
D_{calcd}, Mg/m^3	1.581	1.369
Reflections collected	12533	20597
Reflections independent (R_{int})	5787 (0.0522)	5761 (0.0467)
Goodness-of-fit on F^2	1.011	1.050
$R(I> 2\sigma I)$	0.0468, 0.1131	0.0511, 0.1409

Table S2. Selected bond lengths (Å) and angles (°) for **1**.

Co(1)-O(1)	2.2790(17)	Co(1)-N(4)	2.1039(18)
Co(1)-N(3)	2.1108(17)	Co(1)-N(1)	2.1461(19)
Co(1)-O(2)	2.1631(18)	Co(1)-O(4)	2.195(2)
Co(1)-O(5)	2.2782(19)	N(4)-Co(1)-N(3)	75.12(7)
N(4)-Co(1)-N(1)	148.95(7)	N(3)-Co(1)-N(1)	74.24(7)
N(4)-Co(1)-O(2)	117.81(7)	N(3)-Co(1)-O(2)	143.34(6)
N(1)-Co(1)-O(2)	85.07(8)	N(4)-Co(1)-O(4)	99.75(8)
N(3)-Co(1)-O(4)	90.94(7)	N(1)-Co(1)-O(4)	85.67(7)
O(2)-Co(1)-O(4)	117.74(8)	N(4)-Co(1)-O(5)	84.09(7)
N(3)-Co(1)-O(5)	136.82(7)	N(1)-Co(1)-O(5)	122.56(7)
O(2)-Co(1)-O(5)	79.84(7)	O(4)-Co(1)-O(5)	55.49(7)
N(4)-Co(1)-O(1)	86.66(7)	N(3)-Co(1)-O(1)	92.23(6)
N(1)-Co(1)-O(1)	89.63(7)	O(2)-Co(1)-O(1)	57.10(6)
O(4)-Co(1)-O(1)	173.40(8)	O(5)-Co(1)-O(1)	124.28(7)

Table S3. Selected bond lengths (Å) and angles (°) for **3**.

Co(1)-O(1)	2.086(3)	Co(1)-N(3)	2.121(3)
Co(1)-O(4)	2.133(2)	Co(1)-N(1)	2.151(3)
Co(1)-N(4)	2.175(2)	Co(1)-N(9)	2.183(3)
O(1)-Co(1)-N(3)	162.43(11)	O(1)-Co(1)-O(4)	84.90(11)
N(3)-Co(1)-O(4)	94.67(10)	O(1)-Co(1)-N(1)	123.40(11)
N(3)-Co(1)-N(1)	74.16(10)	O(4)-Co(1)-N(1)	94.78(10)
O(1)-Co(1)-N(4)	88.41(11)	N(3)-Co(1)-N(4)	74.03(10)
O(4)-Co(1)-N(4)	87.04(10)	N(1)-Co(1)-N(4)	148.18(10)
O(1)-Co(1)-N(9)	87.40(11)	N(3)-Co(1)-N(9)	92.19(10)
O(4)-Co(1)-N(9)	172.14(10)	N(1)-Co(1)-N(9)	90.79(10)
N(4)-Co(1)-N(9)	91.15(10)		

Table S4. Experimentally determined LogP values for **1**-**3**.

Co(II) complex	LogP
1	0.94 ± 0.33
2	1.91 ± 0.12
3	1.03 ± 0.02

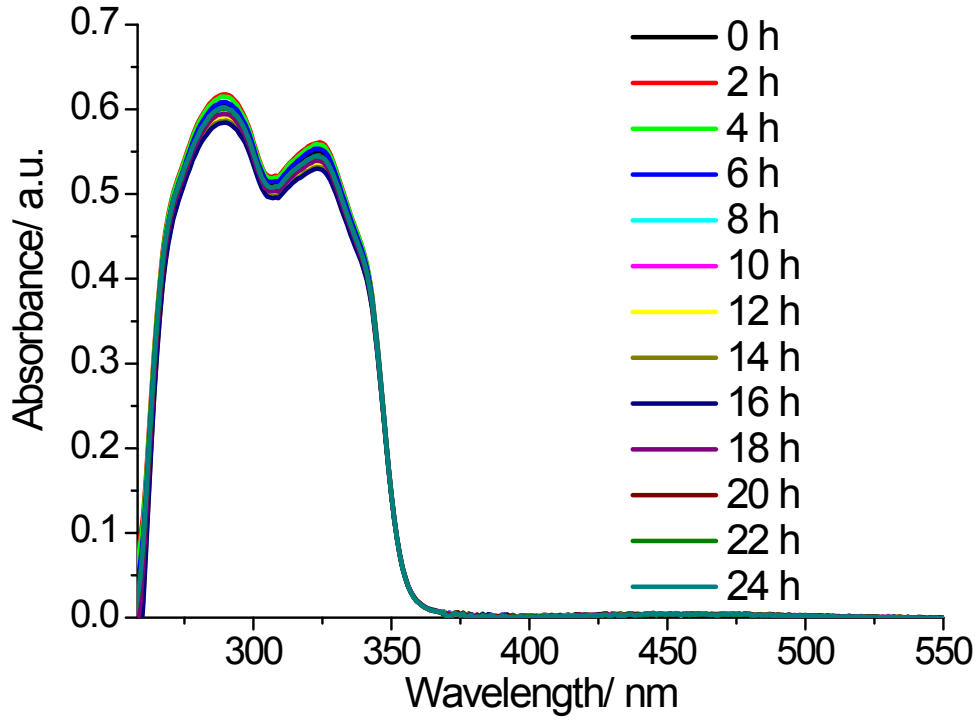

Fig. S6 UV-vis spectrum of **2** (25 μM) in DMSO over the course of 24 h at 37 °C.

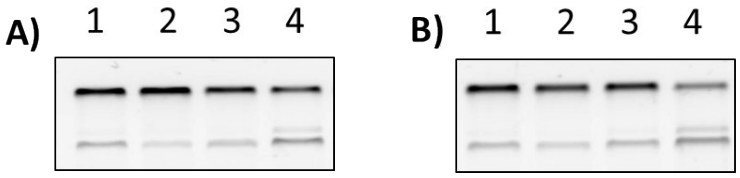

Fig. S7 Concentration-dependent DNA cleavage by **1** and **3** after a 16 h incubation period. (A) Lane 1: DNA only; Lane 2-4: DNA + 1, 5, and 10 μM of **1**; (B) Lane 1: DNA only; Lane 2-4: DNA + 1, 5, and 10 μM of **3**.

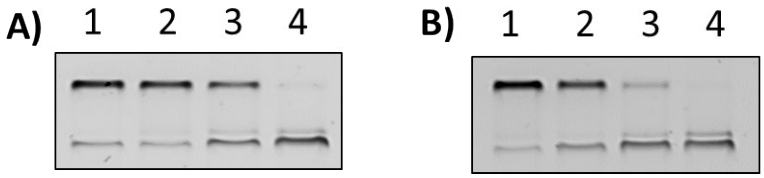

Fig. S8 Effect of ascorbic acid on **1**- and **3**-mediated DNA cleavage after 16 h incubation, (A) Lane 1: DNA only, Lane 2-4: DNA + 1, 5, and 10 μM of **1** with 10 equivalents of ascorbic acid. (B) Lane 1: DNA only, Lane 2-4: DNA + 1, 5, and 10 μM of **3** with 10 equivalents of ascorbic acid.

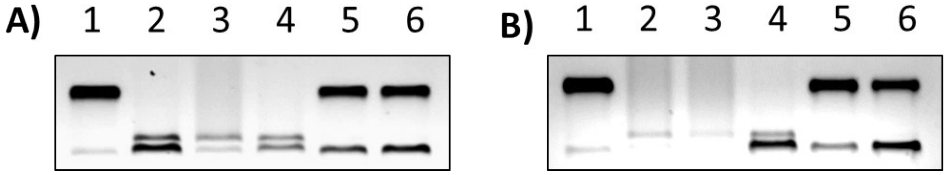

Fig. S9 Inhibition of **1**- and **3**-mediated DNA cleavage by ROS scavengers after 16 h incubation. (A) Lane 1: DNA only, Lane 2: DNA + **1** (10 μM) with 10 equivalents of ascorbic acid, Lane 3-6: DNA + **1** (10 μM) with 10 equivalents of ascorbic acid + NaN_3 (40 mM), KI (40 mM), DMSO (10 mM), or ^{t}BuOH (10 mM). (B) Lane 1: DNA only, Lane 2: DNA + **3** (10 μM) with 10 equivalents of ascorbic acid, Lane 3-6: DNA + **3** (10 μM) with 10 equivalents of ascorbic acid + NaN_3 (40 mM), KI (40 mM), DMSO (10 mM), or ^{t}BuOH (10 mM).

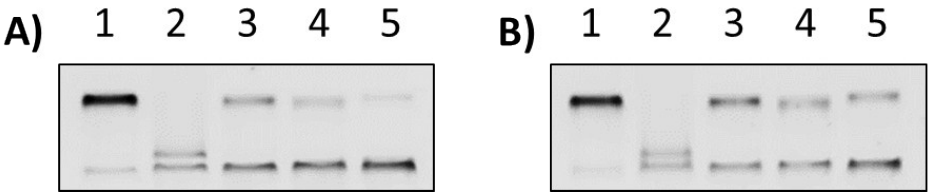

Fig. S10 Inhibition of **1**- and **3**-mediated DNA cleavage by DNA minor and major groove binders and intercalators after 16 h incubation. (A) Lane 1: DNA only, Lane 2: DNA + **1** (10 μM) with 10 equivalents of ascorbic acid, Lane 3: DNA + **1** (10 μM) with 10 equivalents of ascorbic acid + methyl green (50 μM), Lane 4: DNA + **1** (10 μM) with 10 equivalents of ascorbic acid + DAPI (50 μM), Lane 5: DNA + **1** (10 μM) with 10 equivalents of ascorbic acid + TO (10 μM). (B) Lane 1: DNA only, Lane 2: DNA + **3** (10 μM) with 10 equivalents of ascorbic acid, Lane 3: DNA + **3** (10 μM) with 10 equivalents of ascorbic acid + methyl green (50 μM), Lane 4: DNA + **3** (10 μM) with 10 equivalents of ascorbic acid + DAPI (50 μM), Lane 5: DNA + **3** (10 μM) with 10 equivalents of ascorbic acid + TO (10 μM).

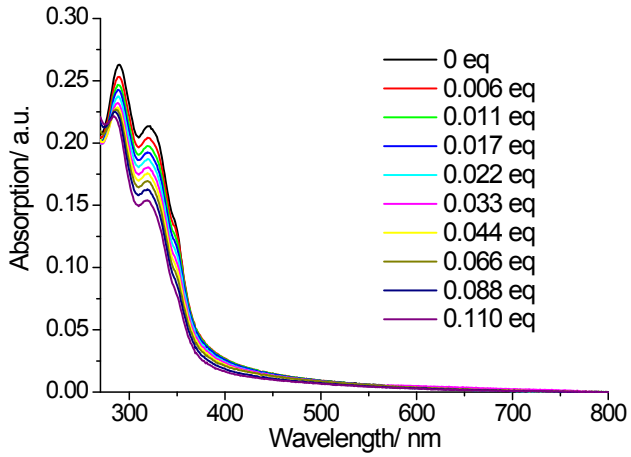

Fig. S11 Representative UV-Vis trace of **1** (50 µM) upon addition of ct-DNA (0 – 0.11 equivalence).

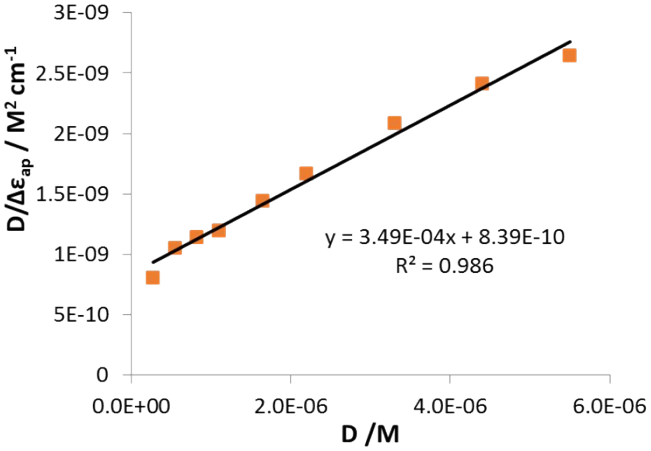

Fig. S12 Representative reciprocal plot of $D/\Delta\varepsilon_{ap}$ versus D of **1** (50 µM) upon addition of ct-DNA (0 – 0.11 eq.).

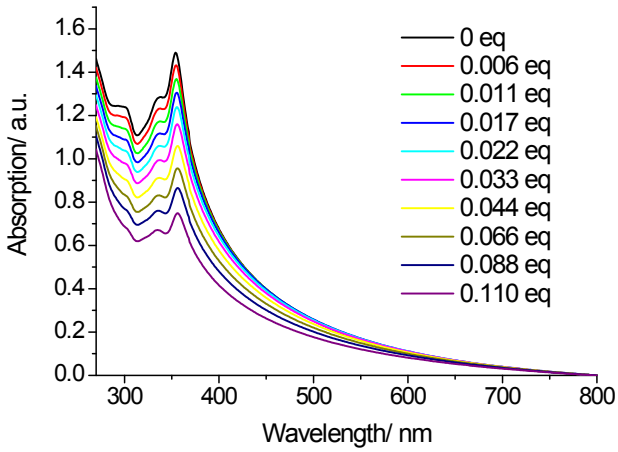

Fig. S13 Representative UV-Vis trace of **3** (50 µM) upon addition of ct-DNA (0 – 0.11 equivalence).

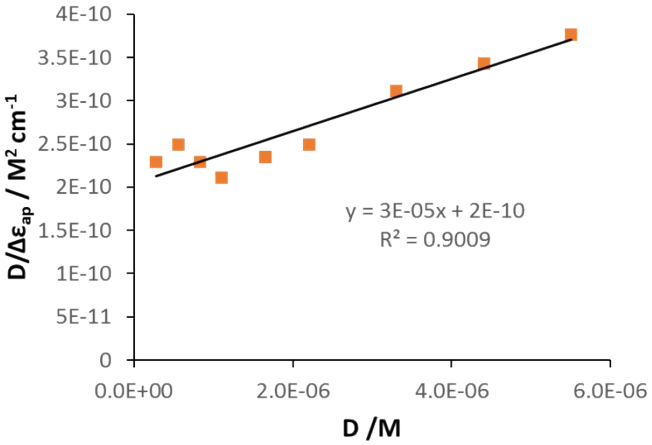

Fig. S14 Representative reciprocal plot of $D/\Delta\varepsilon_{ap}$ versus D of **3** (50 µM) upon addition of ct-DNA (0 – 0.11 eq.).

Table S5. Apparent binding constant (K_{bin}) and quenching constant (K_q) for the interaction of **1-3** with ct-DNA.

Co(II) complex	K_{bin}/ M^{-1}	K_q/ M^{-1}
1	$4.20 \pm 0.05 \times 10^5$	$3.11 \pm 0.14 \times 10^4$
2	$3.70 \pm 0.01 \times 10^5$	$4.92 \pm 0.29 \times 10^4$
3	$1.42 \pm 0.11 \times 10^5$	$5.27 \pm 0.33 \times 10^4$

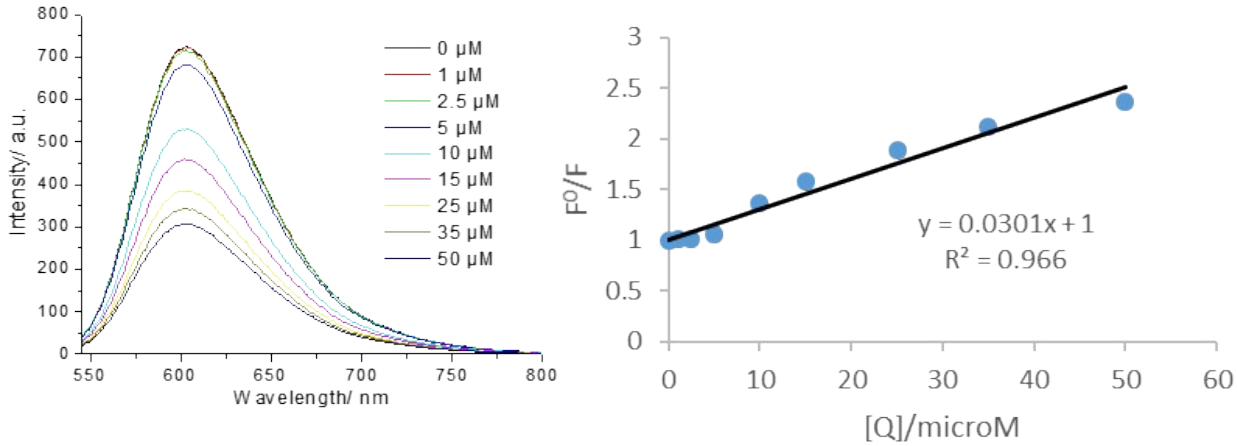

Fig. S15 Emission spectra for ethidium bromide (1 µM) bound to ct-DNA (20 µM) upon addition of aliquots of **1** (0-50 µM) and the corresponding F^o/F versus [Q] plot.

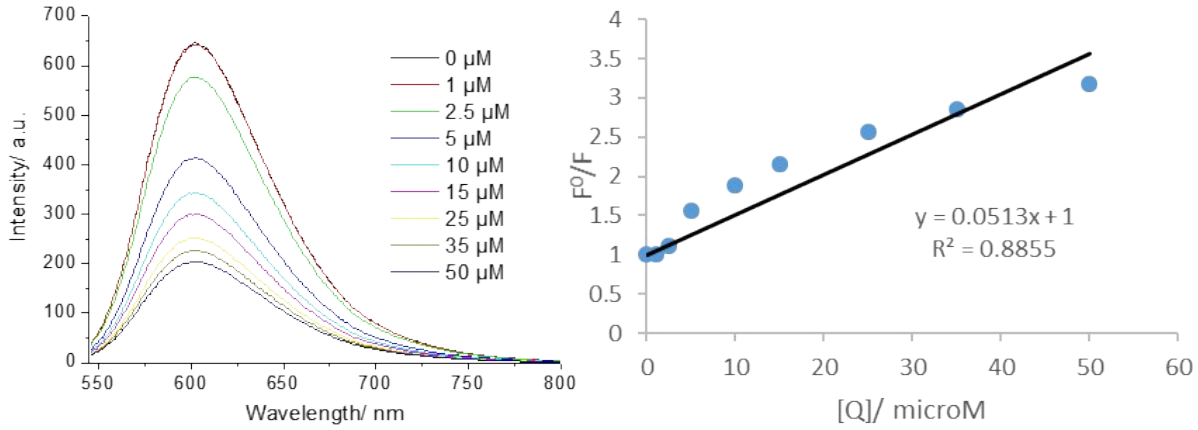

Fig. S16 Emission spectra for ethidium bromide (1 µM) bound to ct-DNA (20 µM) upon addition of aliquots of **2** (0-50 µM) and the corresponding F°/F versus [Q] plot.

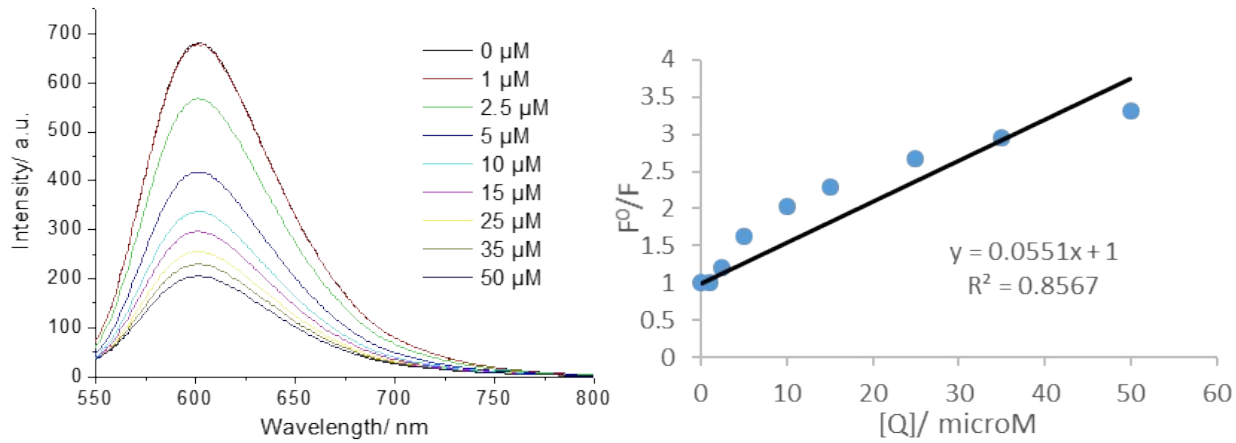

Fig. S17 Emission spectra for ethidium bromide (1 µM) bound to ct-DNA (20 µM) upon addition of aliquots of **3** (0-50 µM) and the corresponding F°/F versus [Q] plot.

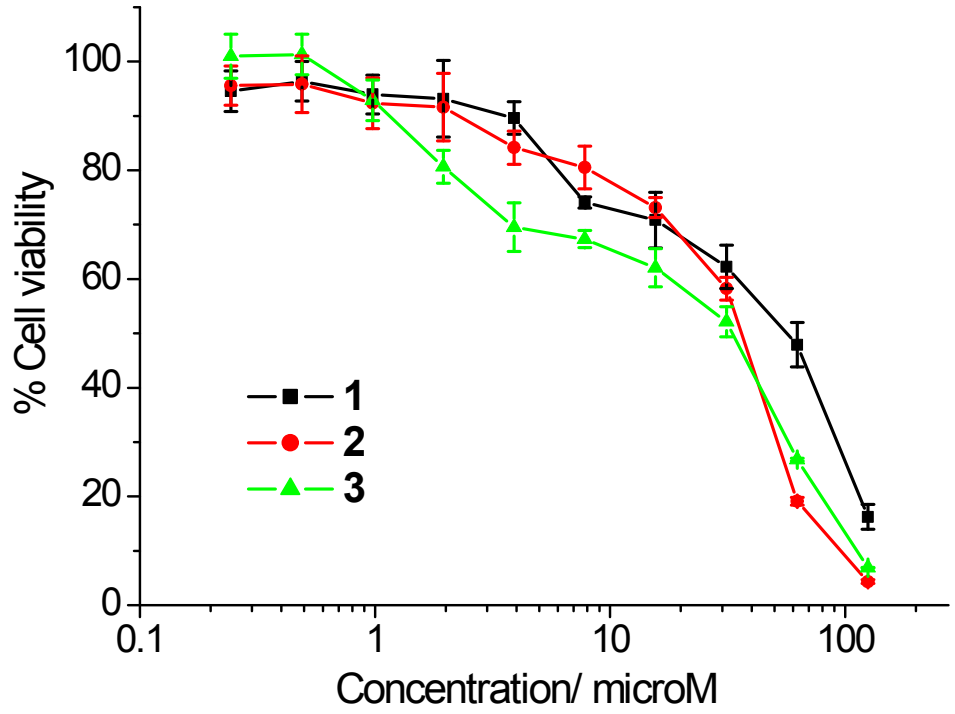

Fig. S18 Representative dose-response curves for the treatment of U2OS cells with **1**-**3** after 72 h incubation.

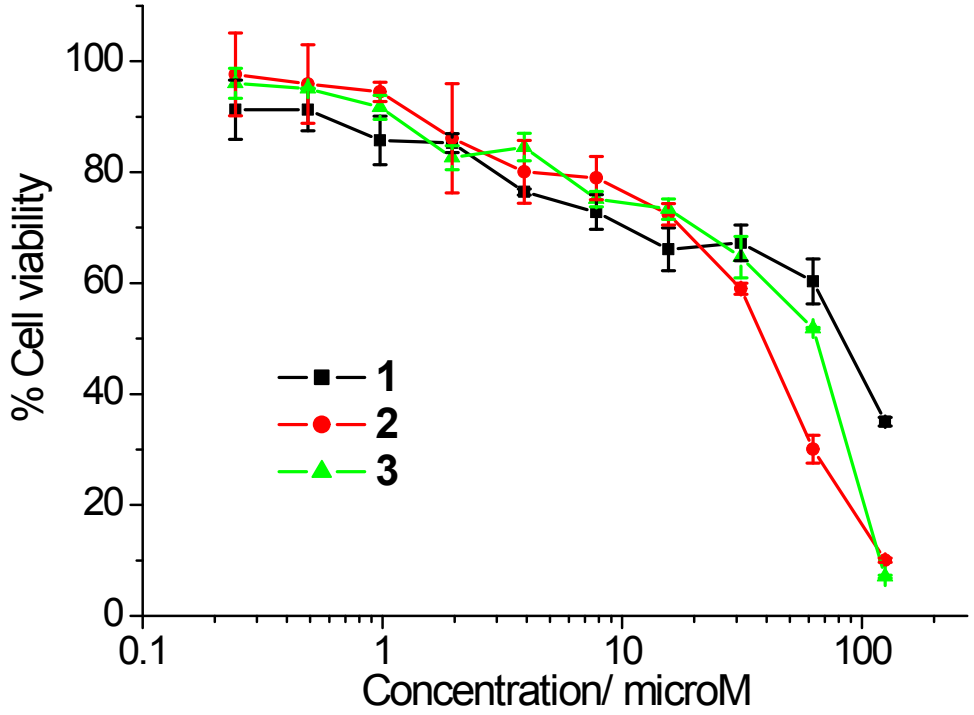

Fig. S19 Representative dose-response curves for the treatment of HepG2 cells with **1**-**3** after 72 h incubation.

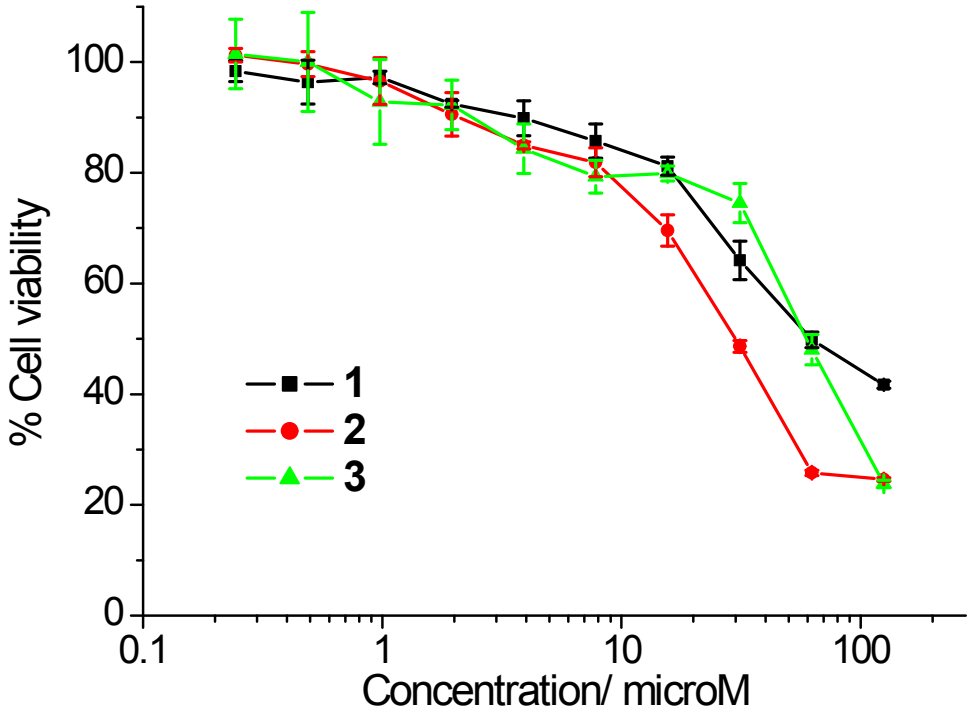

Fig. S20 Representative dose-response curves for the treatment of GM07575 cells with **1**-**3** after 72 h incubation.

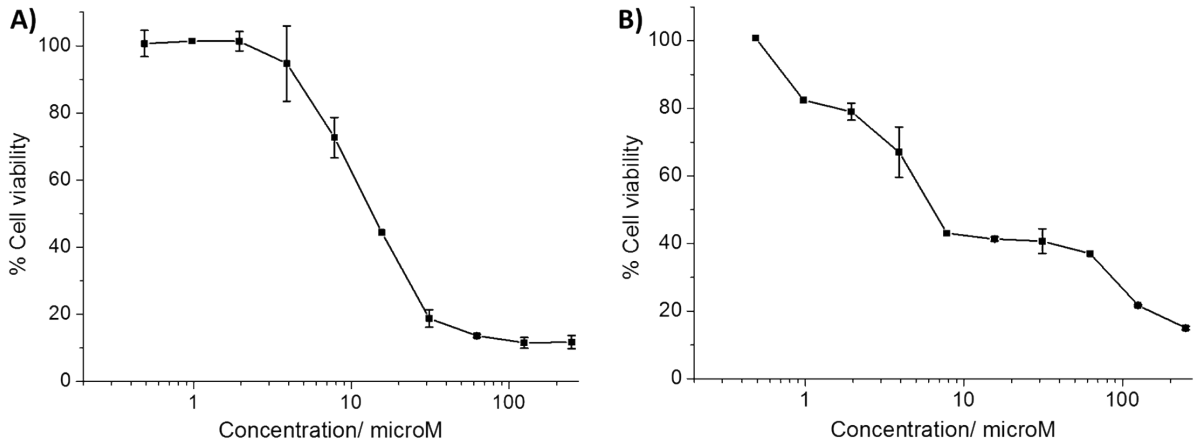

Fig. S21 Representative dose-response curves for the treatment of (A) U2OS or (B) HepG2 cells with cisplatin after 72 h incubation.

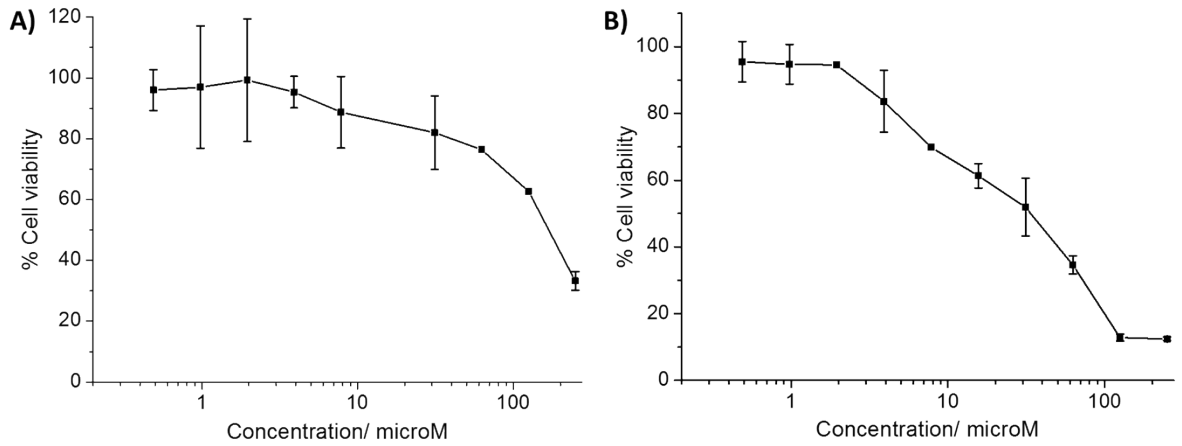

Fig. S22 Representative dose-response curves for the treatment of (A) U2OS or (B) HepG2 cells with carboplatin after 72 h incubation.

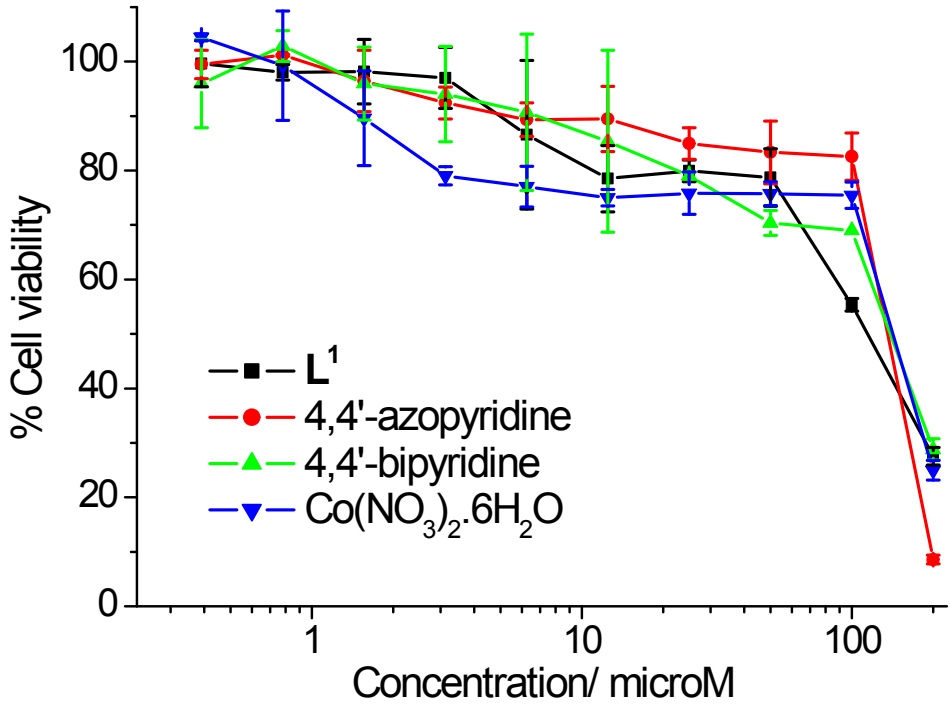

Fig. S23 Representative dose-response curves for the treatment of U2OS cells with $\mathbf{L}^1$, 4,4′-azopyridine, 4,4'-bipyridine, and $Co(NO_3)_2 \cdot 6H_2O$ after 72 h incubation.

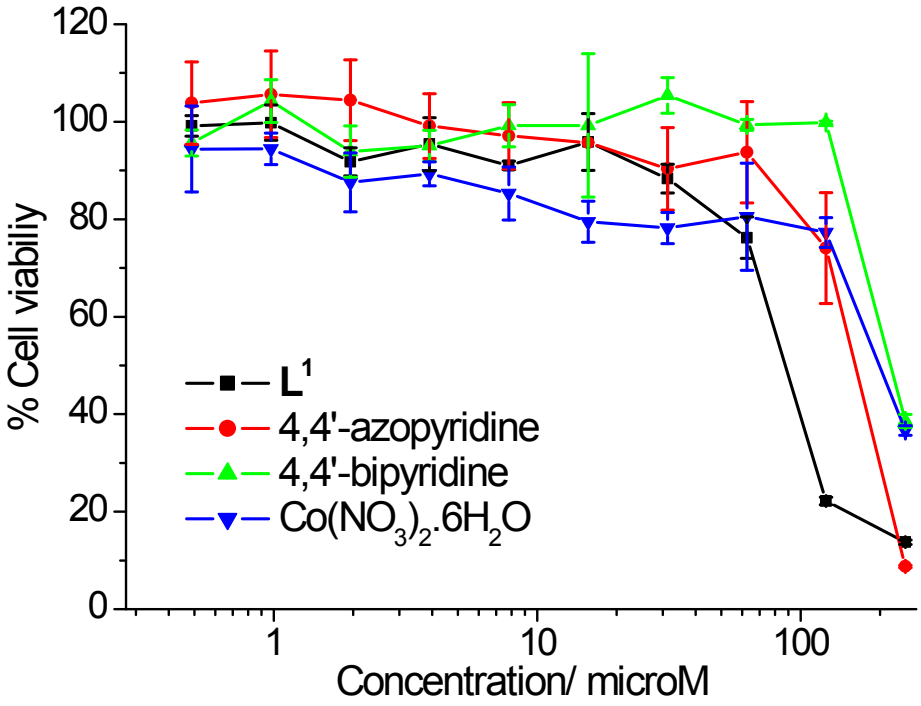

Fig. S24 Representative dose-response curves for the treatment of HepG2 cells with **L**[1], 4,4′-azopyridine, 4,4'-bipyridine, and $Co(NO_3)_2 \cdot 6H_2O$ after 72 h incubation.

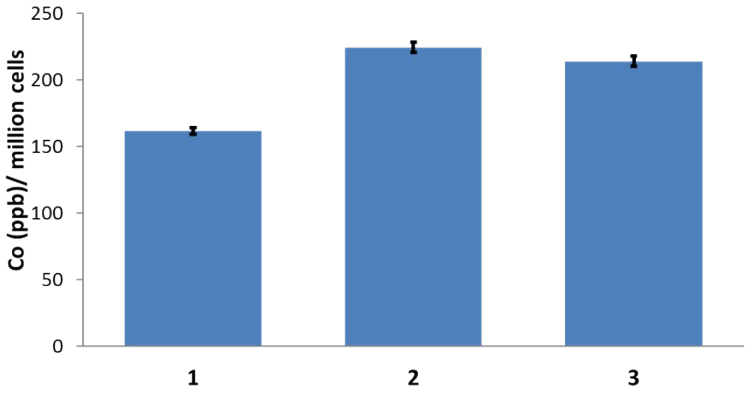

Fig. S25 Cobalt content in U2OS cells treated with **1-3** (10 μM for 24 h).

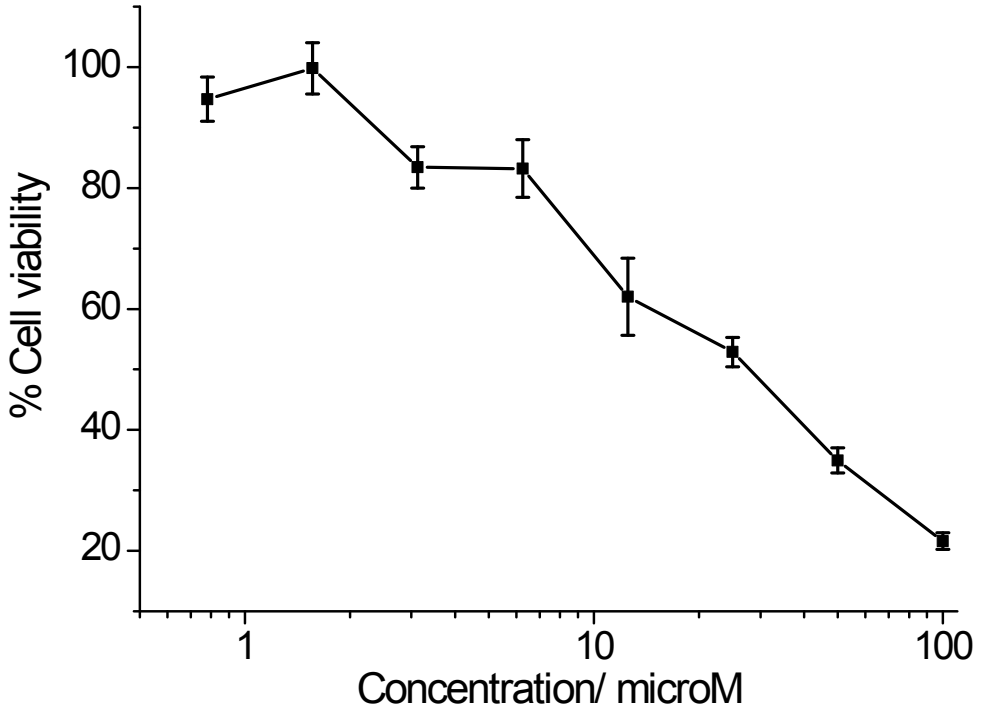

Fig. S26 Representative dose-response curves for the treatment of U2OS cells with **2** in the presence of the p53 inhibitor, pifithrin-μ (10 μM) after 72 h incubation.

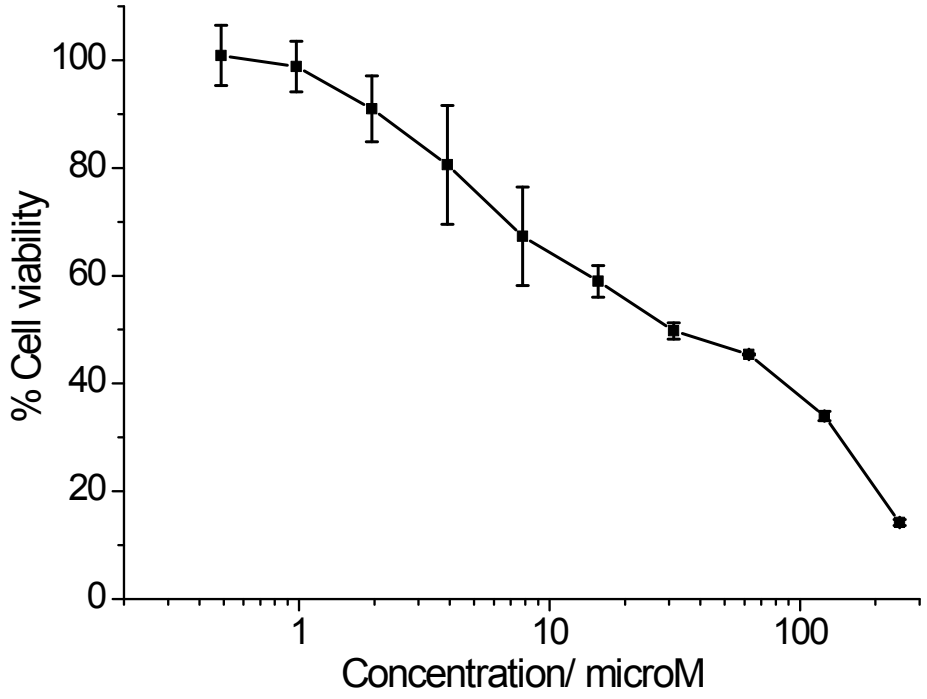

Fig. S27 Representative dose-response curves for the treatment of HepG2 cells with **2** in the presence of the p53 inhibitor, pifithrin-μ (10 μM) after 72 h incubation.